

Isotope Fractionation from *In Vivo* Methylmercury Detoxification in Waterbirds

Brett A. Poulin,* Sarah E. Janssen, Tylor J. Rosera, David P. Krabbenhoft, Collin A. Eagles-Smith, Joshua T. Ackerman, A. Robin Stewart, Eunhee Kim, Zofia Baumann, Jeong-Hoon Kim, and Alain Manceau*



Cite This: *ACS Earth Space Chem.* 2021, 5, 990–997



Read Online

ACCESS |



Metrics & More



Article Recommendations



Supporting Information

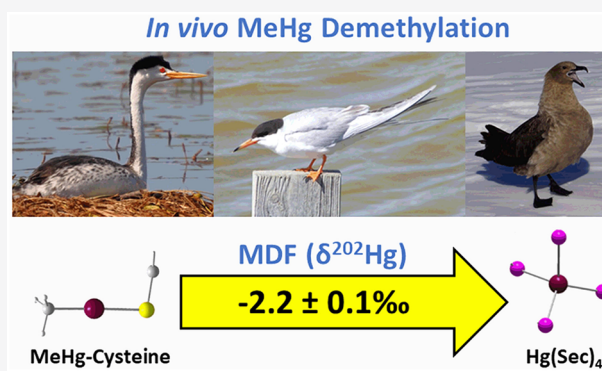
ABSTRACT: The robust application of stable mercury (Hg) isotopes for mercury source apportionment and risk assessment necessitates the understanding of mass-dependent fractionation (MDF) as a result of internal transformations within organisms. Here, we used high energy-resolution X-ray absorption near edge structure spectroscopy and isotope ratios of total mercury ($\delta^{202}\text{THg}$) and methylmercury ($\delta^{202}\text{MeHg}$) to elucidate the chemical speciation of Hg and the resultant MDF as a result of internal MeHg demethylation in waterbirds. In three waterbirds (Clark's grebe, Forster's tern, and south polar skua), between 17 and 86% of MeHg was demethylated to inorganic mercury (iHg) species primarily in the liver and kidneys as Hg–tetraselenolate [$\text{Hg}(\text{Sec})_4$] and minor Hg–dithiolate [$\text{Hg}(\text{SR})_2$] complexes. Tissue differences between $\delta^{202}\text{THg}$ and $\delta^{202}\text{MeHg}$ correlated linearly with %iHg [$\text{Hg}(\text{Sec})_4 + \text{Hg}(\text{SR})_2$] and were interpreted to reflect a kinetic isotope effect during *in vivo* MeHg demethylation. The product–reactant isotopic enrichment factor ($\epsilon_{p/r}$) for the demethylation of MeHg \rightarrow $\text{Hg}(\text{Sec})_4$ was $-2.2 \pm 0.1\text{‰}$. $\delta^{202}\text{MeHg}$ values were unvarying within each bird, regardless of $\text{Hg}(\text{Sec})_4$ abundance, indicating fast internal cycling or replenishment of MeHg relative to demethylation. Our findings document a universal selenium-dependent demethylation reaction in birds, provide new insights on the internal transformations and cycling of MeHg and $\text{Hg}(\text{Sec})_4$, and allow for mathematical correction of $\delta^{202}\text{THg}$ values as a result of the MeHg \rightarrow $\text{Hg}(\text{Sec})_4$ reaction.

KEYWORDS: mercury, demethylation, isotopes, MDF, birds

INTRODUCTION

Mercury (Hg) is a neurotoxin that impacts the health of aquatic and terrestrial animals worldwide.¹ Higher trophic level organisms (e.g., birds, fish, and mammals) are exposed to methylmercury (MeHg) through dietary sources, which is assimilated in the digestive tract, circulated in the bloodstream, and retained in the protein of tissues as a MeHg–cysteine complex (MeHg–Cys).^{2–4} The toxicological risks of MeHg to aquatic and terrestrial organisms are governed by *in vivo* transformations, intertissue exchanges, and depuration rates and pathways of MeHg and other biologically relevant forms of mercury.¹ In birds, MeHg can be demethylated in the liver,^{5,6} depurated into feathers during molt or to offspring by maternal transfer,⁷ and excreted.¹ Stable isotope ratios of mercury are a central tool for ecologic risk assessment and mercury source apportionment to organisms,^{8–14} yet critical questions remain on the isotopic fractionation of mercury by *in vivo* transformations.

The *in vivo* demethylation of MeHg induces mass-dependent fractionation (MDF) of mercury isotopes (denoted by $\delta^{202}\text{Hg}$) as reported in birds,⁶ fish,¹⁵ and mammals.^{9,16–18} The



development^{19,20} and application^{16,17} of methods for species-specific mercury isotope ratio measurements show promise for determining the effect of *in vivo* transformations on mercury isotope ratios. However, a chief barrier is quantifying the chemical speciation of inorganic Hg (iHg) with high precision in natural tissues. High energy-resolution X-ray absorption near-edge structure (HR-XANES) spectroscopy can identify and quantify mixtures of biologically relevant mercury species at subparts per million concentrations.^{3,4,21–23} Recent application of HR-XANES in terrestrial bird and freshwater fish tissues revealed that MeHg–Cys is detoxified to a Hg–tetraselenolate [$\text{Hg}(\text{Sec})_4$] complex, likely by selenoprotein P (SelP).⁴ $\text{Hg}(\text{Sec})_4$ was shown to be the organic precursor to

Received: February 22, 2021

Revised: March 29, 2021

Accepted: April 1, 2021

Published: April 8, 2021



nanoparticulate HgSe,⁴ which has been observed with Hg(Sec)₄ by HR-XANES in marine birds²² and normal resolution XANES in birds and mammals.^{24–26} Linking the chemical speciation of iHg (that indicates specific internal reactions) and MDF of stable mercury isotopes is needed to inform on the internal transformations and redistribution of mercury.

Here, tissues and feathers of piscivorous waterbirds from lacustrine (Clark's grebe, *Aechmophorus clarkia*),^{4,27} estuarine (Forster's tern, *Sterna forsteri forsteri*),²⁸ and marine (south polar skua, *Stercorarius maccormicki*) environments were measured for mercury speciation by HR-XANES spectroscopy and species-specific isotope ratios. Previous research indicates internal MeHg demethylation in these birds.^{4,5} Study goals were to determine the product–reactant isotopic enrichment factor ($\epsilon_{p/r}$) for the *in vivo* detoxification of MeHg to Hg(Sec)₄ and investigate the internal cycling of biologically relevant mercury species. The findings are discussed in context of MeHg detoxification in vertebrates and implications of *in vivo* MDF of mercury isotopes on environmental isotope applications.

MATERIALS AND METHODS

Biological Tissues. Tissues and feathers from three birds were analyzed, including a Clark's grebe (*A. clarkia*; adult male) from Lake Berryessa (California, U.S.A.; collected September 11, 2012), a Forster's tern (*S. forsteri forsteri*; adult female) from the south San Francisco Bay (California, U.S.A.; collected June 13, 2018), and a south polar skua (*S. maccormicki*; adult female) from Cape Hallett located in the northern Victoria Land coast of the Ross Sea (Antarctica; collected November 22, 2016). The Clark's grebe and Forster's tern were necropsied to obtain the following tissues: breast feather, brain, pectoral muscle, kidneys, and liver. The south polar skua was necropsied to obtain the muscle, kidneys, and liver. Tissues were lyophilized and homogenized. Clark's grebe tissues were analyzed previously for mercury speciation by HR-XANES and mercury and selenium association with selenoproteins.⁴

HR-XANES Measurements. HR-XANES spectra of the Clark's grebe tissues are published^{4,29} and were measured identically during the same experimental session on the Forster's tern and south polar skua samples. The south polar skua kidney tissue was not measured by HR-XANES. Complete details are provided in the Supporting Information. Briefly, mercury L₃-edge HR-XANES spectra were measured on freeze-dried samples with high-reflectivity analyzer crystals³⁰ (beamline ID26, European Synchrotron Radiation Facility). Proportions of Hg were quantified using least squares fitting of data with linear combinations of diverse reference spectra.^{4,21,22} The reference spectrum of MeHg–Cys was represented using the Clark's grebe breast feather spectrum, which was suitable based on a spectral comparison to previously analyzed biological samples with exclusively MeHg–Cys.⁴ The spectrum of Hg(Sec)₄ was determined by iterative transformation factor analysis.⁴ The spectrum of Hg–dithiolate [Hg(SR)₂] complex in biota³ was represented using Hg(L-glutathione)₂ at pH 7.4.^{31,32}

Chemical and Isotope Analyses. Details on chemical and isotope measurements are provided in the Supporting Information. Briefly, tissues and feathers were measured for total mercury (THg), MeHg, and total selenium concentrations.³³ Stable mercury isotope ratios were measured on

THg acid digests^{11,12} and resin-separated MeHg fractions²⁰ of all samples from the Clark's grebe and Forster's tern. For the south polar skua, THg isotope ratios were measured on all tissues (muscle, kidneys, and liver) and the MeHg fraction of the kidneys. Isotope analyses were performed using a multicollector inductively coupled plasma mass spectrometer following established protocols^{34,35} on material previously exposed to the X-ray beam for HR-XANES analysis, which had no effect on mercury isotope ratios (Figure S1 of the Supporting Information). Delta values of MDF and mass-independent fractionation (MIF) are expressed as $\delta^{XXX}\text{Hg}$ and $\Delta^{XXX}\text{Hg}$, respectively, in reference to NIST 3133. Isotopic data on certified reference materials and standards are provided in Table S1 of the Supporting Information.

RESULTS AND DISCUSSION

Mercury Speciation in Tissues. The Hg L₃-edge HR-XANES spectra from the three birds show distinct and consistent shifts among tissues that are diagnostic of differences in mercury speciation (Figure 1). The Clark's grebe tissues exhibit the most dramatic differences with mercury present as 100% MeHg–Cys in the brain (indicated by the sharp near-edge peak at 12,279.8 eV unique to MeHg–Cys)^{23,36} and a progressive decrease in the amplitude of the near-edge MeHg–Cys peak in the muscle, kidneys, and liver spectra. As detailed previously,⁴ spectral shifts in the Clark's grebe tissues are due to an increasing percentage of mercury as Hg(Sec)₄ (0, 11, 59, and 86% in brain, muscle, kidneys, and liver, respectively; Table 1 and Table S2 of the Supporting Information). A minor component of the Hg–dithiolate complex [Hg(SR)₂] is observed in the muscle (23%) and kidneys (12%) (Table 1). In the Forster's tern, mercury is present solely as MeHg–Cys in the brain and muscle (100% MeHg–Cys), and the kidneys and liver exhibit increasing proportions of mercury as Hg(Sec)₄ [85% MeHg–Cys + 15% Hg(Sec)₄ and 75% MeHg–Cys + 25% Hg(Sec)₄, respectively; Table 1]. Similarly, the south polar skua shows comparable differences between muscle (100% MeHg–Cys) and liver tissues [83% MeHg–Cys + 17% Hg(Sec)₄]. There is no spectroscopic evidence for nanoparticulate HgSe, as observed in southern giant petrel by HR-XANES.²² All tissues were modeled with high precision (Table S2 of the Supporting Information) as a result of excellent species resolution of HR-XANES (e.g., see reference spectra in Figure 1). Good agreement is observed between %MeHg–Cys measured by HR-XANES and %MeHg measured by chemical measurements (Figure S2 of the Supporting Information), consistent with a previous comparison.⁴

The iHg speciation correlates with the THg concentration between bird tissues. For the Clark's grebe and Forster's tern, THg concentrations of tissues (muscle, kidneys, and liver) were normalized to that of the brain, which exhibited 100% MeHg–Cys. A robust positive correlation is observed between %Hg(Sec)₄ and the relative THg concentration of each tissue to the brain (Figure S3 of the Supporting Information). Molar concentrations of Se to Hg as Hg(Sec)₄ [Se/Hg(Sec)₄ ratio] are >4 in the Forster's tern kidneys and liver and south polar skua liver, consistent with the spectroscopic evidence that tissues contain Hg(Sec)₄ (Figure S4 of the Supporting Information). The Clark's grebe kidneys and liver tissues exhibit $1 < \text{Se}/\text{Hg}(\text{Sec})_4 < 4$, suggesting the co-presence of mononuclear Hg(Sec)₄ complexes and disordered Hg_x(Se,Sec)_y clusters.⁴

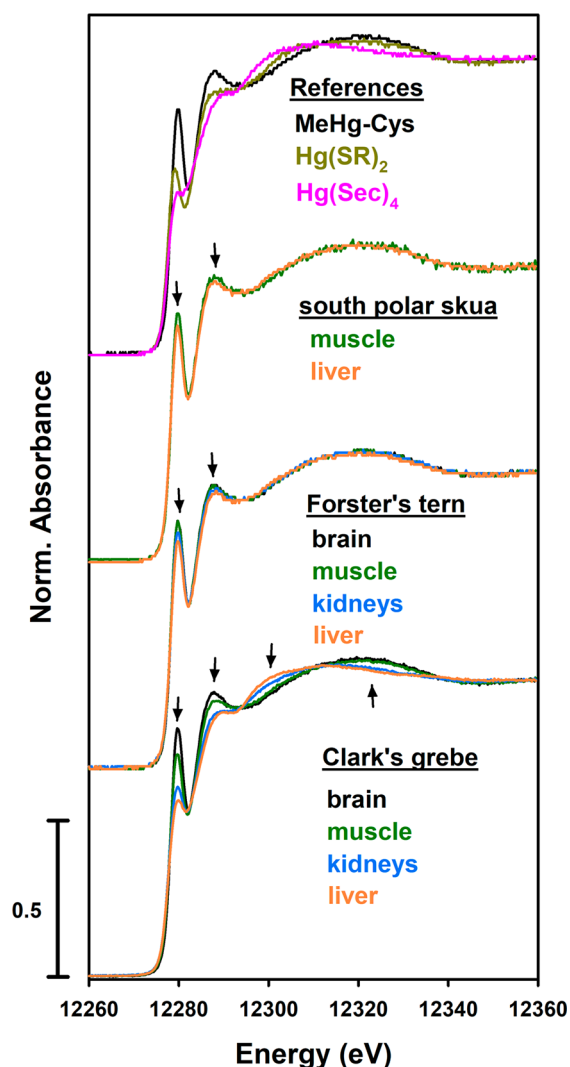


Figure 1. Hg L₃-edge HR-XANES spectra of tissues from a Clark's grebe, Forster's tern, and south polar skua (brain, black; muscle, green; kidneys, blue; and liver, orange). Black arrows identify regions of the spectra that differ with shifts in mercury speciation primarily in the proportion of MeHg-Cys and Hg(Sec)₄. Reference spectra are shown for the three species observed in the tissues [MeHg-Cys, Hg(SR)₂, and Hg(Sec)₄].

MDF via Biotic Demethylation. Mercury isotope ratios showed clear evidence for MDF in tissues that have a mixture of MeHg-Cys and iHg species [Hg(Sec)₄ and Hg(SR)₂] (Figure 2a, Table 1, and Tables S3 and S4 of the Supporting Information). Tissular differences between $\delta^{202}\text{THg}$ and $\delta^{202}\text{MeHg}$ linearly correlated with the %MeHg-Cys (and hence $100 - \%i\text{Hg}$), as determined by HR-XANES (Figure 2a), suggesting that variation in $\delta^{202}\text{THg}$ is the result of mixing of two isotope endmembers ($\delta^{202}\text{MeHg}$ and $\delta^{202}i\text{Hg}$). For the Clark's grebe and Forster's tern, $\delta^{202}\text{THg}$ and $\delta^{202}\text{MeHg}$ were measured on each tissue (Table 1). For the south polar skua, $\delta^{202}\text{THg}$ was measured on the muscle and liver and both $\delta^{202}\text{THg}$ and $\delta^{202}\text{MeHg}$ were measured on the kidneys. The south polar skua kidneys $\delta^{202}\text{MeHg}$ ($1.25 \pm 0.02\text{‰}$) matched the muscle $\delta^{202}\text{THg}$ ($\delta^{202}\text{THg} = 1.25 \pm 0.10\text{‰}$; 100% MeHg-Cys) and, therefore, was representative of $\delta^{202}\text{MeHg}$ in the muscle and liver. Differences between $\delta^{202}\text{THg}$ and $\delta^{202}\text{MeHg}$ were greatest in the Clark's grebe tissues ($\delta^{202}\text{THg} - \delta^{202}\text{MeHg} = -1.90, -1.55, \text{ and } -0.91\text{‰}$ for the liver, kidneys,

and muscle, respectively), followed by Forster's tern liver and kidneys tissues (-0.59 and -0.28‰ , respectively) and the south polar skua liver (-0.45‰). In the Forster's tern, a modest difference was observed between $\delta^{202}\text{THg}$ and $\delta^{202}\text{MeHg}$ values of the muscle (0.22‰), despite no evidence of demethylation, and $\delta^{202}\text{MeHg}$ of the liver was within 0.08‰ of $\delta^{202}\text{THg}$ of the muscle. Although the Clark's grebe muscle and kidneys contained varying proportions of Hg(SR)₂ and Hg(Sec)₄, $\delta^{202}\text{Hg}$ values were consistently light compared to $\delta^{202}\text{MeHg}$ and statistically align with the regression line between $\delta^{202}\text{THg} - \delta^{202}\text{MeHg}$ versus %MeHg-Cys (Figure 2a and Figure S5 of the Supporting Information) of tissues where Hg(Sec)₄ is the dominant iHg species. Therefore, $\delta^{202}i\text{Hg}$ is considered representative of the dominant Hg(Sec)₄ species.

Within each bird, variations of $\Delta^{199}\text{Hg}$ values and $\Delta^{199}\text{Hg}/\Delta^{201}\text{Hg}$ ratios for both the THg and MeHg fractions were largely within measurement precision, regardless of mercury speciation (Figure 2b, Table 1, and Figure S6 of the Supporting Information), consistent with previous observations of the absence of MIF during internal partitioning and transformations of Hg within organisms.^{6,9,17,18} The uniformity in $\Delta^{199}\text{Hg}$ and slope of $\Delta^{199}\text{Hg}/\Delta^{201}\text{Hg}$ between the MeHg and iHg species indicate that photochemical demethylation occurs within the food web prior to dietary assimilation of MeHg and likely reflects the prey habitat and foraging behavior of the birds.^{13,14,37,38}

We interpret isotopic differences between MeHg and Hg(Sec)₄ to be the result of a kinetic isotope effect during the *in vivo* demethylation of MeHg \rightarrow Hg(Sec)₄. $\delta^{202}\text{MeHg}$ exhibited little variation within the Clark's grebe ($-0.05 \pm 0.18\text{‰}$, average \pm standard deviation; $n = 4$) and Forster's tern ($0.49 \pm 0.14\text{‰}$; $n = 4$), regardless of differences in mercury speciation (Table 1 and Figure 2b). Therefore, the isotopic fractionation of mercury in the birds behaved as an open system with an infinite reservoir of reactant (i.e., MeHg). Assuming a unidirectional reaction and instantaneous product,³⁹ the product-reactant isotopic enrichment factor [$\epsilon_{\text{Hg}(\text{Sec})_4/\text{MeHg}}$] was determined as the y intercept of the linear regression between $\delta^{202}\text{THg} - \delta^{202}\text{MeHg}$ versus %MeHg-Cys [$\epsilon_{\text{Hg}(\text{Sec})_4/\text{MeHg}} = -2.2 \pm 0.1\text{‰}$, slope \pm 95% confidence interval of fit; Figure 2a]. The linear regression weighted each data point to measurement uncertainties.⁴⁰ MDF of mercury likely occurs during demethylation of MeHg to Hg(Sec)₄, likely by SelP. SelP is rich in selenocysteine residues ($n \geq 10$ for vertebrates)^{4,41} that can facilitate MeHg demethylation^{42,43} and was associated with Hg(Sec)₄ and Hg_x(Se,Sec)_y in the Clark's grebe tissues.⁴ Notably, the Clark's grebe kidneys and muscle tissues contained Hg(SR)₂ along with Hg(Sec)₄. Consistent MDF of tissues that contain Hg(SR)₂ and Hg(Sec)₄ and those with only Hg(Sec)₄ support that Hg(SR)₂ is also a byproduct of *in vivo* demethylation of MeHg (Figure 2a and Figure S5 of the Supporting Information), although through an unknown pathway. Provided that Hg(Sec)₄ is spectroscopically indistinguishable from Hg_x(Se,Sec)_y, as observed in the grebe liver and kidneys, the MDF for the demethylation reaction could result from demethylation of MeHg to Hg_x(Se,Sec)_y.

We report the first isotopic enrichment factor for *in vivo* demethylation of MeHg by selenium in vertebrates. The magnitude of $\epsilon_{\text{Hg}(\text{Sec})_4/\text{MeHg}}$ in birds ($-2.2 \pm 0.1\text{‰}$) is similar to isotopic differences observed in a range of aquatic mammals (detailed below) but markedly greater than the microbial *mer*

Table 1. Chemical, Spectroscopic, and Isotopic Data of Bird Tissue and Feather Samples

tissue	chemical measurements ^a			HR-XANES fit results ^b			species-specific isotope ratios			
	THg (mg/kg)	MeHg (mg/kg)	Se (mg/kg)	%MeHg-Cys	%Hg(Sec) ₄	%Hg(SR) ₂	$\delta^{202}\text{THg}$ (± 1 SD)	$\Delta^{199}\text{THg}$ (± 1 SD)	$\delta^{202}\text{MeHg}$ (± 1 SD)	$\Delta^{199}\text{MeHg}$ (± 1 SD)
Clark's grebe (<i>A. clarkii</i>)										
brain	3.18	2.98	1.55	100	0	0	0.07 (0.03)	1.51 (0.03)	0.06 (0.04)	1.49 (0.02)
muscle	7.10	3.71	2.31	66	11	23	-1.13 (0.04)	1.46 (0.04)	-0.22 (0.03)	1.43 (0.02)
kidneys	21.6	6.38	10.6	28	59	12	-1.41 (0.03)	1.42 (0.04)	0.14 (0.02)	1.45 (0.03)
liver	43.1	7.86	19.3	14	86	0	-2.07 (0.04)	1.49 (0.04)	-0.17 (0.02)	1.42 (0.02)
breast feather	41.4	32.7	1.04	100	0	0	0.15 (0.03)	1.77 (0.02)	0.13 (0.05)	2.04 (0.03)
Forster's tern (<i>S. forsteri</i>)										
brain	5.28	4.48	3.31	100	0	0	0.51 (0.02)	0.68 (0.02)	0.57 (0.01)	0.81 (0.02)
muscle	6.39	5.65	3.33	100	0	0	0.53 (0.03)	0.72 (0.03)	0.31 (0.02)	0.79 (0.02)
kidneys	12.6	9.21	9.64	85	15	0	0.34 (0.02)	0.70 (0.03)	0.62 (0.03)	0.66 (0.02)
liver	13.8	9.22	6.21	75	25	0	-0.14 (0.02)	0.67 (0.03)	0.45 (0.04)	0.71 (0.08)
breast feather	28.6	18.2	1.41	100	0	0	0.70 (0.03)	1.65 (0.04)	0.72 (0.02)	1.81 (0.04)
south polar skua (<i>S. maccormicki</i>)										
muscle	1.75	1.39	19.4	100	0	0	1.25 (0.05)	1.99 (0.03)		
kidneys	8.61	4.56					0.17 (0.03)	2.00 (0.05)	1.25 (0.01)	1.92 (0.01)
liver	8.19	6.39	29.7	83	17	0	0.80 (0.01)	2.02 (0.04)		

^aReported on a dry weight basis. ^bPrecision of fit results are 5% for the Clark's grebe tissues⁴ and 10% for Forster's tern and south polar skua tissues (see Table S2 of the Supporting Information).

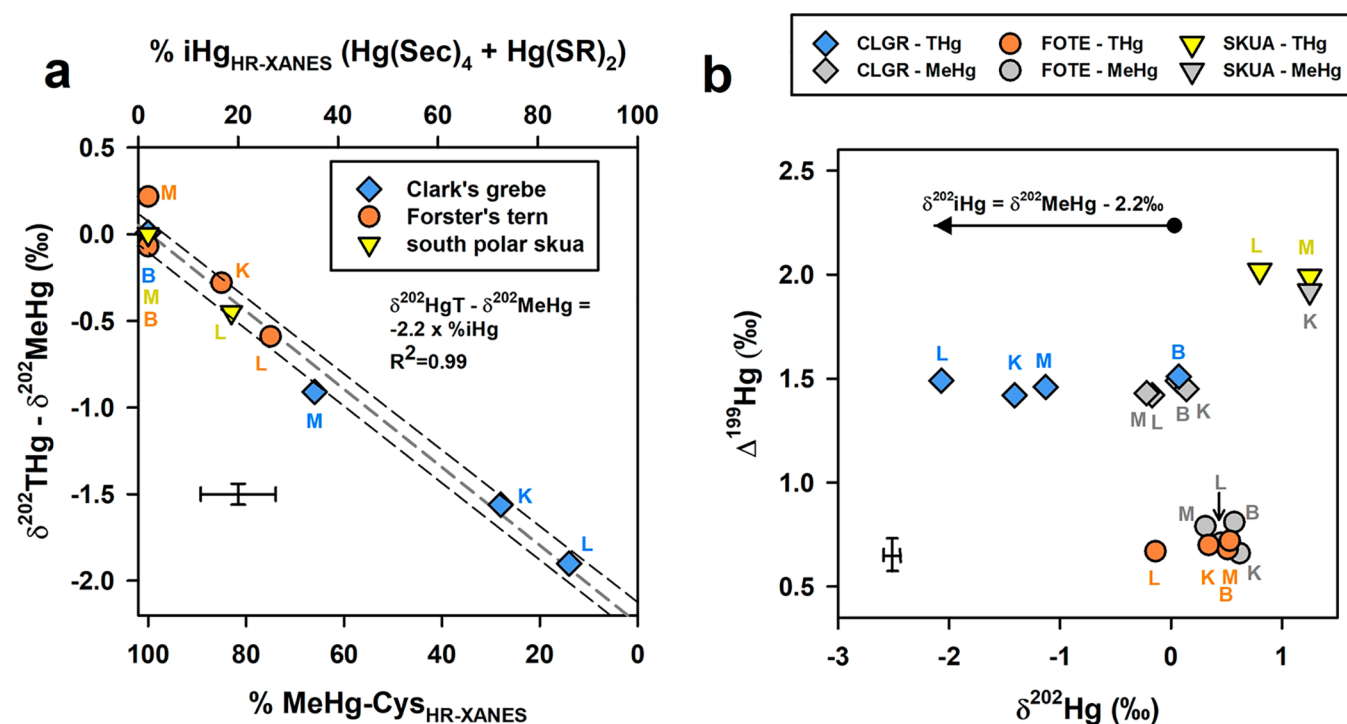


Figure 2. (a) Relationship between the difference in $\delta^{202}\text{Hg}$ values of total mercury minus methylmercury ($\delta^{202}\text{THg} - \delta^{202}\text{MeHg}$; Table 1) and the speciation of mercury as determined by HR-XANES of bird tissues; data are weighted to uncertainties of both x and y variables. (b) Biplot of $\Delta^{199}\text{Hg}$ versus $\delta^{202}\text{Hg}$ of total mercury (THg; color-filled symbols) and methylmercury (MeHg; gray-filled symbols) for bird tissues. Single letters identify the tissue type (B, brain; K, kidneys; L, liver; and M, muscle). Generic error bars present uncertainties of isotope measurements (2 SD) and HR-XANES fits (Table S2 of the Supporting Information). In panel a, the dashed gray and black lines present the fit of data and 95% confidence interval of the fit, respectively.

pathway ($\epsilon_{p/r} = -0.40 \pm 0.20\text{‰}$).⁴⁴ In mammal tissues where species-specific isotopic ratios were determined ($\delta^{202}\text{MeHg}$ and $\delta^{202}\text{THg}$),^{16,17} differences between $\delta^{202}\text{MeHg}$ and $\delta^{202}\text{iHg}$ pools were estimated to range from -2.1 to $\sim -3\text{‰}$ (beluga whale and freshwater seal¹⁶ muscle versus liver and pilot whale brain tissues).¹⁷ In a study where only $\delta^{202}\text{THg}$ was measured,¹⁸ the maximum difference in $\delta^{202}\text{THg}$ between

muscle ($\sim 100\%$ MeHg) and liver ($\sim 6\%$ MeHg) in juvenile pilot whales was $\sim -2.3\text{‰}$. Consistent MDF by MeHg demethylation across birds and mammals could be explained by a universal reaction mechanism involving Selp,⁴ which is central to selenium homeostasis.⁴¹ A more detailed comparison of $\epsilon_{\text{Hg}(\text{Sec})_4/\text{MeHg}}$ to isotope measurements of other birds,⁶ fish,^{15,19,20} or mammals^{9,16-18} would require species-specific

isotope ratios and HR-XANES speciation, and knowledge of possible isotope effects from poorly understood processes [e.g., biomineralization of nanoparticulate HgSe from $\text{Hg}(\text{Sec})_4$].^{22,24} The expression of selenoproteins and insertion efficiency of selenocysteine residues during protein translation can vary between organisms, between tissues, and based on selenium availability,^{41,45} and may influence the extent of MeHg demethylation across different organisms⁶ and associated isotopic fractionation in environments that differ in selenium availability. Future research efforts are needed to evaluate the mechanisms and isotopic fractionation for MeHg demethylation by SelP, other selenoproteins,⁴⁶ and low-molecular-weight selenium-containing molecules,⁴⁷ and quantify the variation in $\epsilon_{\text{Hg}(\text{Sec})_4/\text{MeHg}}$ across diverse organisms and environmental settings (e.g., terrestrial versus marine).

Complementary spectroscopic and isotopic findings shed new light on the toxicokinetics of mercury in birds. With regard to MeHg, tissular $\delta^{202}\text{MeHg}$ values were not influenced by the local kinetic isotopic effect for the $\text{MeHg} \rightarrow \text{Hg}(\text{Sec})_4$ reaction (Figure 2b and Table 1) as would be predicted in a closed system. This observation likely reflects the fast internal cycling of MeHg relative to the demethylation reaction, consistent with observations in birds⁶ and marine mammals,^{16,17} and dilution of residual heavy $\delta^{202}\text{MeHg}$ with new dietary MeHg. The $\delta^{202}\text{MeHg}$ values of the Clark's grebe and Forster's tern feathers, which fingerprint blood mercury isotope ratios during feather growth,⁴⁸ were within the narrow range of tissular $\delta^{202}\text{MeHg}$ values (Table 1). Internal exchange of MeHg leading to uniform $\delta^{202}\text{MeHg}$ in the birds is consistent with the dynamic nature of MeHg levels in birds as a result of physiological (e.g., molting and age) and environmental factors (e.g., dietary exposure).^{10,27,28,49}

With regard to the toxicokinetics of $\text{Hg}(\text{Sec})_4$, the correlation between tissular concentrations of THg and $\% \text{Hg}(\text{Sec})_4$ (Figure S3 of the Supporting Information) indicates that $\text{Hg}(\text{Sec})_4$ is depurated considerably slower than MeHg, consistent with observations between fish muscle versus liver.⁴ It is unclear if $\text{Hg}(\text{Sec})_4$ and $\text{Hg}(\text{SR})_2$ in non-hepatic tissues were demethylated locally or are the result of intertissular exchange. Intertissular exchange of $\text{Hg}(\text{Sec})_4$ or $\text{Hg}(\text{SR})_2$ cannot be discounted, has been proposed in birds^{6,22} and mammals,^{16–18} and is represented in toxicokinetic models,⁵⁰ but there is a lack of mechanistic studies in nature. More broadly, *in vivo* demethylation of MeHg has been attributed to positive MDF between dietary MeHg and organism MeHg.^{9,17,38,51,52} Quantifying the contribution of $\text{MeHg} \rightarrow \text{Hg}(\text{Sec})_4$ or $\text{Hg}(\text{SR})_2$ on MDF between dietary and organism MeHg cannot be carried out here and necessitates an improved mechanistic understanding of isotopic fractionation from additional processes (e.g., ligand exchange⁵³ and $\text{Hg}(\text{Sec})_4 \rightarrow$ nanoparticulate HgSe biomineralization).²² Toxicokinetic models for mercury in birds⁵⁴ and mammals⁵⁰ will benefit from advancements from emerging techniques described here and elsewhere^{4,20,22} that provide a foundation to understand the transformations and redistribution of biologically relevant mercury species [MeHg , $\text{Hg}(\text{SR})_2$, $\text{Hg}(\text{Sec})_4$, and nanoparticulate HgSe].

Implications on Environmental Applications of Stable Mercury Isotope Ratios. This study demonstrates significant MDF of mercury in bird tissues as a result of the demethylation of MeHg to primarily $\text{Hg}(\text{Sec})_4$.⁴ $\delta^{202}\text{MeHg}$ values were relatively unaffected by MeHg demethylation, and

therefore, direct measurement of $\delta^{202}\text{MeHg}$ on tissues²⁰ is recommended for use of $\delta^{202}\text{Hg}$ for contaminant source apportionment^{8–11} in higher trophic level organisms and on liver or kidney tissues that are not predominantly MeHg.^{1,6,9,17,18} It is unknown if isotopically light products of *in vivo* demethylation [$\text{Hg}(\text{Sec})_4$ and $\text{Hg}(\text{SR})_2$] are transferred within foodwebs (e.g., scavenging of high trophic level organisms at the base of foodwebs).^{13,20} Where direct isotopic analysis of the MeHg pool is not feasible, mathematical correction of $\delta^{202}\text{THg}$ using $\epsilon_{\text{Hg}(\text{Sec})_4/\text{MeHg}}$ may be warranted in determining the isotopic composition of dietary MeHg sources prior to *in vivo* demethylation. When applying the $\epsilon_{\text{Hg}(\text{Sec})_4/\text{MeHg}}$ ($-2.2 \pm 0.1\%$), spectroscopic characterization of tissues is encouraged under two scenarios. First, in tissues with high %MeHg (e.g., >80%), HR-XANES analysis should be used to accurately quantify %MeHg as a result of incomplete recovery of MeHg using traditional chemical techniques (Figure S2 of the Supporting Information, Figure S4 of the Supporting Information in the study by Manceau et al.,⁴ and Figure S2 of the Supporting Information in the study by Bolea-Fernandez et al.¹⁸). Second, in tissues with low %MeHg (e.g., <30%), HR-XANES analysis is necessary to detect co-occurrence of $\text{Hg}(\text{Sec})_4$ and nanoparticulate HgSe.²² It remains unknown if the biomineralization of nanoparticulate HgSe from $\text{Hg}(\text{Sec})_4$ induces positive or negative MDF based on the observation in marine bird⁶ and mammal tissues with very low %MeHg.^{16–18,24}

■ ASSOCIATED CONTENT

Supporting Information

The Supporting Information is available free of charge at <https://pubs.acs.org/doi/10.1021/acsearthspacechem.1c00051>.

Descriptions of measurements, mercury isotope ratios for CRMs, standards, and samples (Tables S1, S3, and S4 and Figures S1 and S6), HR-XANES spectra fit results (Table S2), comparison of %MeHg by HR-XANES and chemical analysis (Figure S2), correlations between the THg concentration and iHg speciation (Figure S3), ratios of Se/Hg (Figure S4), and comparison of isotope versus $\% \text{Hg}(\text{Sec})_4$ by HR-XANES results (Figure S5) (PDF)
HR-XANES spectra (XLSX)

■ AUTHOR INFORMATION

Corresponding Authors

Brett A. Poulin – Department of Environmental Toxicology, University of California Davis, Davis, California 95616, United States; U.S. Geological Survey, Water Mission Area, Boulder, Colorado 80303, United States; orcid.org/0000-0002-5555-7733; Phone: +1-530-754-2454; Email: bapoulin@ucdavis.edu

Alain Manceau – University Grenoble Alpes, ISTERre, CNRS, 38058 Grenoble, France; orcid.org/0000-0003-0845-611X; Email: alain.manceau@univ-grenoble-alpes.fr

Authors

Sarah E. Janssen – U.S. Geological Survey, Upper Midwest Water Science Center, Middleton, Wisconsin 53562, United States; orcid.org/0000-0003-4432-3154

Taylor J. Rosera – U.S. Geological Survey, Upper Midwest Water Science Center, Middleton, Wisconsin 53562, United States

States; Environmental Chemistry and Technology Program, University of Wisconsin—Madison, Madison, Wisconsin 53706, United States

David P. Krabbenhoft — U.S. Geological Survey, Upper Midwest Water Science Center, Middleton, Wisconsin 53562, United States; orcid.org/0000-0003-1964-5020

Collin A. Eagles-Smith — U.S. Geological Survey, Forest and Rangeland Ecosystem Science Center, Corvallis, Oregon 97331, United States; orcid.org/0000-0003-1329-5285

Joshua T. Ackerman — U.S. Geological Survey, Western Ecological Research Center, Dixon Field Station, Dixon, California 95620, United States; orcid.org/0000-0002-3074-8322

A. Robin Stewart — U.S. Geological Survey, Water Mission Area, Menlo Park, California 94025, United States

Eunhee Kim — Citizens' Institute for Environmental Studies (CIES), Seoul 110-761, Korea

Zofia Baumann — Department of Marine Sciences, University of Connecticut, Groton, Connecticut 06340, United States

Jeong-Hoon Kim — Division of Life Sciences, Korea Polar Research Institute, Incheon 21990, Korea

Complete contact information is available at:

<https://pubs.acs.org/10.1021/acsearthspacechem.1c00051>

Notes

The authors declare no competing financial interest.

ACKNOWLEDGMENTS

The authors thank Pieter Glatzel, Blanka Detlefs (European Synchrotron Radiation Facility), and Kathryn Nagy (University of Illinois at Chicago) for support during data collection on beamline ID26. The authors thank Mike Tate, Jake Ogorek, John Pierce, and Caitlin Rumrill (U.S. Geological Survey) for assistance with mercury isotope and concentration measurements. The authors acknowledge Brooke Hill, Jeong-Hoon Kim, and Josh Ackerman for photos of Forster's tern, south polar skua, and Clark's grebe used in the table of contents (TOC) art. The authors thank Ryan Lepak (U.S. Environmental Protection Agency) and two anonymous reviewers for constructive feedback on the manuscript. Financial support was provided to Brett A. Poulin by the U.S. National Science Foundation under Grant EAR-1629698, to Brett A. Poulin, Sarah E. Janssen, A. Robin Stewart, David P. Krabbenhoft, Collin A. Eagles-Smith, and Joshua T. Ackerman by the U.S. Geological Survey (USGS) Environmental Health Mission Area's Toxic Substances Hydrology and Contaminants Biology Programs, and to A. Robin Stewart by the Water Mission Area. Financial support was provided to Alain Manceau by the French National Research Agency (ANR) under Grant ANR-10-EQPX-27-01 (EcoX Equipex) and to Eunhee Kim and Jeong-Hoon Kim by the Ecosystem Structure and Function of Marine Protected Area (MPA) in Antarctica Project (PM20060), funded by the Ministry of Oceans and Fisheries (20170336), Korea. Any use of trade, firm, or product names is for descriptive purposes only and does not imply endorsement by the U.S. Government.

REFERENCES

(1) Chételat, J.; Ackerman, J. T.; Eagles-Smith, C. A.; Hebert, C. E. Methylmercury exposure in wildlife: A review of the ecological and physiological processes affecting contaminant concentrations and their interpretation. *Sci. Total Environ.* **2020**, *711*, 135117.

(2) Harris, H. H.; Pickering, I. J.; George, G. N. The chemical form of mercury in fish. *Science* **2003**, *301*, 1203.

(3) Bourdineaud, J. P.; Gonzalez-Rey, M.; Rovezzi, M.; Glatzel, P.; Nagy, K. L.; Manceau, A. Divalent mercury in dissolved organic matter is bioavailable to fish and accumulates as dithiolate and tetrathiolate complexes. *Environ. Sci. Technol.* **2019**, *53*, 4880–4891.

(4) Manceau, A.; Bourdineaud, J. P.; Oliveira, R. B.; Sarrazin, S. L. F.; Krabbenhoft, D. P.; Eagles-Smith, C. A.; Ackerman, J. T.; Stewart, A. R.; Ward-Deitrich, C.; del Castillo Busto, M. E.; Goenaga-Infante, H.; Wack, A.; Retegan, M.; Detlefs, B.; Glatzel, P.; Bustamante, P.; Nagy, K. L.; Poulin, B. A. Demethylation of methylmercury in bird, fish, and earthworm. *Environ. Sci. Technol.* **2021**, *55*, 1527–1534.

(5) Eagles-Smith, C. A.; Ackerman, J. T.; Yee, J.; Adelsbach, T. L. Mercury demethylation in waterbird livers: Dose-response thresholds and differences among species. *Environ. Toxicol. Chem.* **2009**, *28*, 568–577.

(6) Renedo, M.; Pedrero, Z.; Amouroux, D.; Cherel, Y.; Bustamante, P. Mercury Isotopes of Key Tissues Document Mercury Metabolic Processes in Seabirds. *Chemosphere* **2021**, *263*, 127777.

(7) Ackerman, J. T.; Herzog, M. P.; Evers, D. C.; Cristol, D. A.; Kenow, K. P.; Heinz, G. H.; Lavoie, R. A.; Brasso, R. L.; Mallory, M. L.; Provencher, J. F.; Braune, B. M.; Matz, A.; Schmutz, J. A.; Eagles-Smith, C. A.; Savoy, L. J.; Meyer, M. W.; Hartman, C. A. Synthesis of maternal transfer of mercury in birds: Implications for altered toxicity risk. *Environ. Sci. Technol.* **2020**, *54*, 2878–2891.

(8) Li, M.; Schartup, A. T.; Valberg, A. P.; Ewald, J. D.; Krabbenhoft, D. P.; Yin, R.; Balcom, P. H.; Sunderland, E. M. Environmental origins of methylmercury accumulated in subarctic estuarine fish indicated by mercury stable isotopes. *Environ. Sci. Technol.* **2016**, *50*, 11559–11568.

(9) Masbou, J.; Sonke, J. E.; Amouroux, D.; Guillou, G.; Becker, P. R.; Point, D. Hg-stable isotope variations in marine top predators of the western Arctic Ocean. *ACS Earth Sp. Chem.* **2018**, *2*, 479–490.

(10) Renedo, M.; Amouroux, D.; Pedrero, Z.; Bustamante, P.; Cherel, Y. Identification of sources and bioaccumulation pathways of MeHg in subantarctic penguins: A stable isotopic investigation. *Sci. Rep.* **2018**, *8*, 8865.

(11) Lepak, R. F.; Janssen, S. E.; Yin, R.; Krabbenhoft, D. P.; Ogorek, J. M.; DeWild, J. F.; Tate, M. T.; Holsen, T. M.; Hurley, J. P. Factors affecting mercury stable isotopic distribution in piscivorous fish of the Laurentian Great Lakes. *Environ. Sci. Technol.* **2018**, *52*, 2768–2776.

(12) Lepak, R. F.; Hoffman, J. C.; Janssen, S. E.; Krabbenhoft, D. P.; Ogorek, J. M.; DeWild, J. F.; Tate, M. T.; Babiarz, C. L.; Yin, R.; Murphy, E. W.; Engstrom, D. R.; Hurley, J. P. Mercury source changes and food web shifts alter contamination signatures of predatory fish from Lake Michigan. *Proc. Natl. Acad. Sci. U. S. A.* **2019**, *116*, 23600–23608.

(13) Blum, J. D.; Drazen, J. C.; Johnson, M. W.; Popp, B. N.; Motta, L. C.; Jamieson, A. J. Mercury isotopes identify near-surface marine mercury in deep-sea trench biota. *Proc. Natl. Acad. Sci. U. S. A.* **2020**, *117*, 29292–29298.

(14) Blum, J. D.; Sherman, L. S.; Johnson, M. W. Mercury isotopes in earth and environmental sciences. *Annu. Rev. Earth Planet. Sci.* **2014**, *42*, 249–269.

(15) Rua-Ibarz, A.; Bolea-Fernandez, E.; Maage, A.; Frantzen, S.; Sanden, M.; Vanhaecke, F. Tracing mercury pollution along the Norwegian coast via elemental, speciation, and isotopic analysis of liver and muscle tissue of deep-water marine fish (*Brosme Brosme*). *Environ. Sci. Technol.* **2019**, *53*, 1776–1785.

(16) Perrot, V.; Masbou, J.; Pastukhov, M. V.; Epov, V. N.; Point, D.; Bérail, S.; Becker, P. R.; Sonke, J. E.; Amouroux, D. Natural Hg isotopic composition of different Hg compounds in mammal tissues as a proxy for in vivo breakdown of toxic methylmercury. *Metallomics* **2016**, *8*, 170.

(17) Li, M.; Juang, C. A.; Ewald, J. D.; Yin, R.; Mikkelsen, B.; Krabbenhoft, D. P.; Balcom, P. H.; Dassuncao, C.; Sunderland, E. M. Selenium and stable mercury isotopes provide new insights into

mercury toxicokinetics in pilot whales. *Sci. Total Environ.* **2020**, *710*, 136325.

(18) Bolea-Fernandez, E.; Rua-Ibarz, A.; Krupp, E. M.; Feldmann, J.; Vanhaecke, F. High-precision isotopic analysis sheds new light on mercury metabolism in long-finned pilot whales (*Globicephala Melas*). *Sci. Rep.* **2019**, *9*, 7262.

(19) Masbou, J.; Point, D.; Sonke, J. E. Application of a selective extraction method for methylmercury compound specific stable isotope analysis (MeHg-CSIA) in biological materials. *J. Anal. At. Spectrom.* **2013**, *28*, 1620–1628.

(20) Rosera, T. J.; Janssen, S. E.; Tate, M. T.; Lepak, R. F.; Ogorek, J. M.; DeWild, J. F.; Babiaryz, C. L.; Krabbenhoft, D. P.; Hurley, J. P. Isolation of methylmercury using distillation and anion-exchange chromatography for isotopic analyses in natural matrices. *Anal. Bioanal. Chem.* **2020**, *412*, 681–690.

(21) Manceau, A.; Bustamante, P.; Haouz, A.; Bourdineaud, J. P.; Gonzalez-Rey, M.; Lemouchi, C.; Gautier-Luneau, I.; Geertsen, V.; Barruet, E.; Rovezzi, M.; Glatzel, P.; Pin, S. Mercury(II) binding to metallothionein in *Mytilus Edulis* revealed by high energy-resolution XANES spectroscopy. *Chem. - Eur. J.* **2019**, *25*, 997.

(22) Manceau, A.; Gaillot, A. C.; Glatzel, P.; Cherel, Y.; Bustamante, P. *In Vivo* formation of HgSe nanoparticles and Hg-tetraselenolate complex from methylmercury in seabird—Implications for the Hg-Se antagonism. *Environ. Sci. Technol.* **2021**, *55*, 1515–1526.

(23) Manceau, A.; Enescu, M.; Simionovici, A.; Lanson, M.; Gonzalez-Rey, M.; Rovezzi, M.; Tucoulou, R.; Glatzel, P.; Nagy, K. L.; Bourdineaud, J. P. Chemical forms of mercury in human hair reveal sources of exposure. *Environ. Sci. Technol.* **2016**, *50*, 10721–10729.

(24) Gajdosechova, Z.; Lawan, M. M.; Urgast, D. S.; Raab, A.; Scheckel, K. G.; Lombi, E.; Kopittke, P. M.; Loeschner, K.; Larsen, E. H.; Woods, G.; Brownlow, A.; Read, F. L.; Feldmann, J.; Krupp, E. M. *In vivo* formation of natural HgSe nanoparticles in the liver and brain of pilot whales. *Sci. Rep.* **2016**, *6*, 34361.

(25) Nakazawa, E.; Ikemoto, T.; Hokura, A.; Terada, Y.; Kunito, T.; Tanabe, S.; Nakai, I. The presence of mercury selenide in various tissues of the striped dolphin: Evidence from μ -XRF-XRD and XAFS analyses. *Metallomics* **2011**, *3*, 719–725.

(26) Arai, T.; Ikemoto, T.; Hokura, A.; Terada, Y.; Kunito, T.; Tanabe, S.; Nakai, I. Chemical forms of mercury and cadmium accumulated in marine mammals and seabirds as determined by XAFS analysis. *Environ. Sci. Technol.* **2004**, *38*, 6468–6474.

(27) Hartman, C. A.; Ackerman, J. T.; Herzog, M. P.; Eagles-Smith, C. A. Season, molt, and body size influence mercury concentrations in grebes. *Environ. Pollut.* **2017**, *229*, 29–39.

(28) Ackerman, J. T.; Eagles-Smith, C. A.; Takekawa, J. Y.; Bluso, J. D.; Adelsbach, T. L. Mercury concentrations in blood and feathers of prebreeding Forster's terns in relation to space use of San Francisco Bay, California, USA, Habitats. *Environ. Toxicol. Chem.* **2008**, *27*, 897–908.

(29) Poulin, B. A.; Manceau, A.; Krabbenhoft, D. P.; Stewart, A. R.; Ward-Deitrich, C.; del Castillo Busto, M. E.; Goenaga-Infante, H.; Bustamante, P. Mercury and selenium chemical characteristics and speciation data of bird, fish, and earthworm tissues. *U.S. Geological Survey Data Release* **2020**, DOI: 10.5066/P96NP376.

(30) Rovezzi, M.; Lapras, C.; Manceau, A.; Glatzel, P.; Verbeni, R. High energy-resolution X-ray spectroscopy at ultra-high dilution with spherically bent crystal analyzers of 0.5 m radius. *Rev. Sci. Instrum.* **2017**, *88*, 013108.

(31) Mah, V.; Jalilehvand, F. Glutathione complex formation with mercury(II) in aqueous solution at physiological pH. *Chem. Res. Toxicol.* **2010**, *23*, 1815–1823.

(32) Manceau, A.; Wang, J.; Rovezzi, M.; Glatzel, P.; Feng, X. Biogenesis of mercury-sulfur nanoparticles in plant leaves from atmospheric gaseous mercury. *Environ. Sci. Technol.* **2018**, *52*, 3935–3948.

(33) Kleckner, A. E.; Kakouros, E.; Robin Stewart, A. A practical method for the determination of total selenium in environmental samples using isotope dilution-hydride generation-inductively coupled

plasma-mass spectrometry. *Limnol. Oceanogr.: Methods* **2017**, *15*, 363–371.

(34) Janssen, S. E.; Lepak, R. F.; Tate, M. T.; Ogorek, J. M.; DeWild, J. F.; Babiaryz, C. L.; Hurley, J. P.; Krabbenhoft, D. P. Rapid pre-concentration of mercury in solids and water for isotopic analysis. *Anal. Chim. Acta* **2019**, *1054*, 95–103.

(35) Yin, R.; Krabbenhoft, D. P.; Bergquist, B. A.; Zheng, W.; Lepak, R. F.; Hurley, J. P. Effects of mercury and thallium concentrations on high precision determination of mercury isotopic composition by Neptune Plus multiple collector inductively coupled plasma mass spectrometry. *J. Anal. At. Spectrom.* **2016**, *31*, 2060–2068.

(36) Thomas, S. A.; Mishra, B.; Myneni, S. C. B. Cellular mercury coordination environment, and not cell surface ligands, influence bacterial methylmercury production. *Environ. Sci. Technol.* **2020**, *54*, 3960–3968.

(37) Bergquist, B. A.; Blum, J. D. Mass-dependent and -independent fractionation of Hg isotopes by photoreduction in aquatic systems. *Science* **2007**, *318*, 417–420.

(38) Perrot, V.; Pastukhov, M. V.; Epov, V. N.; Husted, S.; Donard, O. F. X.; Amouroux, D. Higher mass-independent isotope fractionation of methylmercury in the pelagic food web of Lake Baikal (Russia). *Environ. Sci. Technol.* **2012**, *46*, 5902–5911.

(39) Mariotti, A.; Germon, J. C.; Hubert, P.; Kaiser, P.; Letolle, R.; Tardieux, A.; Tardieux, P. Experimental determination of nitrogen kinetic isotope fractionation: Some principles; illustration for the denitrification and nitrification processes. *Plant Soil* **1981**, *62*, 413–430.

(40) York, D. Least-squares fitting of a straight line. *Can. J. Phys.* **1966**, *44*, 1079–1086.

(41) Burk, R. F.; Hill, K. E. Selenoprotein P-expression, functions, and roles in mammals. *Biochim. Biophys. Acta, Gen. Subj.* **2009**, *1790*, 1441–1447.

(42) Khan, M. A. K.; Wang, F. Chemical demethylation of methylmercury by selenoamino acids. *Chem. Res. Toxicol.* **2010**, *23*, 1202–1206.

(43) Asaduzzaman, A. M.; Schreckenbach, G. Degradation mechanism of methyl mercury selenoamino acid complexes: A computational study. *Inorg. Chem.* **2011**, *50*, 2366–2372.

(44) Kritee, K.; Barkay, T.; Blum, J. D. Mass dependent stable isotope fractionation of mercury during mer mediated microbial degradation of monomethylmercury. *Geochim. Cosmochim. Acta* **2009**, *73*, 1285–1296.

(45) Penglase, S.; Hamre, K.; Ellingsen, S. The selenium content of SEPP1 versus selenium requirements in vertebrates. *PeerJ* **2015**, *3*, e1244.

(46) Pickering, I. J.; Cheng, Q.; Rengifo, E. M.; Nehzati, S.; Dolgova, N. V.; Kroll, T.; Sokaras, D.; George, G. N.; Arnér, E. S. J. Direct observation of methylmercury and auranofin binding to selenocysteine in thioredoxin reductase. *Inorg. Chem.* **2020**, *59*, 2711–2718.

(47) Yamashita, Y.; Yamashita, M. Identification of a novel selenium-containing compound, selenoneine, as the predominant chemical form of organic selenium in the blood of bluefin tuna. *J. Biol. Chem.* **2010**, *285*, 18134–18138.

(48) Renedo, M.; Amouroux, D.; Duval, B.; Carravieri, A.; Tessier, E.; Barre, J.; Béral, S.; Pedrero, Z.; Cherel, Y.; Bustamante, P. Seabird tissues as efficient biomonitoring tools for Hg isotopic investigations: Implications of using blood and feathers from chicks and adults. *Environ. Sci. Technol.* **2018**, *52*, 4227–4234.

(49) Seewagen, C. L.; Cristol, D. A.; Gerson, A. R. Mobilization of mercury from lean tissues during simulated migratory fasting in a model songbird. *Sci. Rep.* **2016**, *6*, 25762.

(50) Ewald, J. D.; Kirk, J. L.; Li, M.; Sunderland, E. M. Organ-specific differences in mercury speciation and accumulation across ringed seal (*Phoca hispida*) life stages. *Sci. Total Environ.* **2019**, *650*, 2013–2020.

(51) Sherman, L. S.; Blum, J. D.; Franzblau, A.; Basu, N. New insight into biomarkers of human mercury exposure using naturally occurring mercury stable isotopes. *Environ. Sci. Technol.* **2013**, *47*, 3403–3409.

(52) Laffont, L.; Sonke, J. E.; Maurice, L.; Monrroy, S. L.; Chincheros, J.; Amouroux, D.; Behra, P. Hg speciation and stable isotope signatures in human hair as a tracer for dietary and occupational exposure to mercury. *Environ. Sci. Technol.* **2011**, *45*, 9910–9916.

(53) Wiederhold, J. G.; Cramer, C. J.; Daniel, K.; Infante, I.; Bourdon, B.; Kretzschmar, R. Equilibrium mercury isotope fractionation between dissolved Hg(II) species and thiol-bound Hg. *Environ. Sci. Technol.* **2010**, *44*, 4191–4197.

(54) Bearhop, S.; Ruxton, G. D.; Furness, R. W. Dynamics of mercury in blood and feathers of great skuas. *Environ. Toxicol. Chem.* **2000**, *19*, 1638–1643.